Conduction Velocity and Anisotropic Properties of Fibrillation Waves During Acutely Induced and Long-Standing Persistent AF

van Schie, Mathijs S.; Talib, Shmaila; Knops, Paul; Taverne, Yannick J.H.J.; de Groot, Natasja M.S.

DOI
10.1016/j.jacep.2024.02.001

Publication date
2024

Document Version
Final published version

Published in
JACC: Clinical Electrophysiology

JACC: CLINICAL ELECTROPHYSIOLOGY VOL. 10, NO. 7, 2024

ORIGINAL RESEARCH

ATRIAL FIBRILLATION - PATHOPHYSIOLOGY

Conduction Velocity and Anisotropic Properties of Fibrillation Waves During Acutely Induced and Long-Standing Persistent AF

Mathijs S. van Schie, MSc,[a] Shmaila Talib, MD, MSc,[b] Paul Knops, BSc,[a] Yannick J.H.J. Taverne, MD, PhD,[c] Natasja M.S. de Groot, MD, PhD[a,d]

ABSTRACT

BACKGROUND Quantified features of local conduction heterogeneity due to pathological alterations of myocardial tissue could serve as a marker for the degree of electrical remodeling and hence be used to determine the stage of atrial fibrillation (AF).

OBJECTIVES In this study, the authors investigated whether local directional heterogeneity (LDH) and anisotropy ratio, derived from estimated local conduction velocities (CVs) during AF, are suitable electrical parameters to stage AF.

METHODS Epicardial mapping (244-electrode array, interelectrode distance 2.25 mm) of the right atrium was performed during acute atrial fibrillation (AAF) (n = 25, 32 ± 11 years of age) and during long-standing persistent atrial fibrillation (LSPAF) (n = 23, 64 ± 9 years of age). Episodes of 9 ± 4 seconds of AF were analyzed. Local CV vectors were constructed to assess the degree of anisotropy. Directions and magnitudes of individual vectors were compared with surrounding vectors to identify LDH.

RESULTS Compared with the entire AAF group, LSPAF was characterized by slower conduction (71.5 ± 6.8 cm/s vs 67.6 ± 5.6 cm/s; $P = 0.037$) with a larger dispersion (1.59 ± 0.21 vs 1.95 ± 0.17; $P < 0.001$) and temporal variability (32.0 ± 4.7 cm/s vs 38.5 ± 3.3 cm/s; $P < 0.001$). Also, LSPAF was characterized by more LDH (19.6% ± 4.4% vs 26.0% ± 3.4%; $P < 0.001$) and a higher degree of anisotropy (1.38 ± 0.07 vs 1.51 ± 0.14; $P < 0.001$). Compared with the most complex type of AAF (type III), LSPAF was still associated with a larger CV dispersion, higher temporal variability of CV, and larger amount of LDH.

CONCLUSIONS Increasing AF complexity was associated with increased spatiotemporal variability of local CV vectors, local conduction heterogeneity, and anisotropy ratio. By using these novel parameters, LSPAF could potentially be discriminated from the most complex type of AAF. These observations may indicate pathological alterations of myocardial tissue underlying progression of AF. (JACC Clin Electrophysiol 2024;10:1592-1604) © 2024 The Authors. Published by Elsevier on behalf of the American College of Cardiology Foundation. This is an open access article under the CC BY license (http://creativecommons.org/licenses/by/4.0/).

From the [a]Department of Cardiology, Erasmus Medical Center, Rotterdam, the Netherlands; [b]Department of Cardiology, Haga Teaching Hospital, The Hague, the Netherlands; [c]Department of Cardiothoracic Surgery, Erasmus Medical Center, Rotterdam, the Netherlands; and the [d]Department of Microelectronics, Delft University of Technology, Delft, the Netherlands.

The authors attest they are in compliance with human studies committees and animal welfare regulations of the authors' institutions and Food and Drug Administration guidelines, including patient consent where appropriate. For more information, visit the Author Center.

Manuscript received October 25, 2023; revised manuscript received February 1, 2024, accepted February 4, 2024.

ISSN 2405-500X https://doi.org/10.1016/j.jacep.2024.02.001

Nonremodeled atrial tissue is considered to be uniform anisotropic in nature, resulting in a faster electrical conduction along the longitudinal direction of myocardial fibers than in the transverse direction.[1] The speed and direction of a propagating wavefront through myocardial tissue is determined by a range of functional and structural properties, such as membrane properties, tissue structure, and wavefront geometry.[1,2] Tissue damage affecting cell-to-cell communication results in a heterogeneous distribution of conduction properties, which is known as nonuniform anisotropy. Nonuniform anisotropic tissue may result in intra-atrial conduction disorders, which play a crucial role in both genesis and perpetuation of tachyarrhythmias such as atrial fibrillation (AF).[3-6]

Although atrial tissue often is considered to be highly anisotropic, in patients without structural heart disease, Hansson et al[7] surprisingly demonstrated that conduction velocity (CV) during stable sinus rhythm at the epicardial right atrial free wall was not dependent on propagation direction. Konings et al[8] showed that during acutely induced, self-terminating AF, the right atrial free wall of young patients without structural heart disease was mainly activated uniformly by broad wavefronts with occasionally arcs of functional conduction block. In the same patients, Houben et al[9] also reported low anisotropic conduction ratios (median 1.2). It is most likely that conduction in older patients with underlying cardiac diseases and dilated atria is additionally affected by alterations of the atrial structure, thereby inducing nonuniform anisotropic features.[3]

Recently, we developed a novel methodology to estimate local CV and accurately identify local conduction heterogeneities during sinus rhythm without smoothing of wavefront propagation.[10] Also, local directional heterogeneity (LDH) in CV vectors was quantified, which could be used as indicator of the degree of electropathology.[11] Hence, LDH could serve as an electrical biomarker to discriminate acutely induced, self-terminating AF from (long-standing) persistent AF. The goal of this study was therefore to apply this novel methodology during AF to quantify directional CV, LDH, and the resulting anisotropy ratio, and to test whether these parameters differ between patients with different types of AF.

METHODS

STUDY POPULATION. For this study, a unique, historical dataset of AF electrograms was used.[8,12] These electrograms were recorded during epicardial mapping studies, which have been performed in 48 patients during open chest surgery. Twenty-five patients (16 male, 32 ± 11 years of age) with Wolff-Parkinson-White syndrome underwent cardiac surgery for interruption of an accessory pathway. In these patients, AF was acutely induced by programmed electrical stimulation (acute atrial fibrillation [AAF] group). All patients had normal sized atria (left atrial diameter 39 ± 6 mm) and no history of valvular heart disease or coronary artery disease. The AAF group was further subdivided according to the degree of complexity of AF into type I (n = 10), II (n = 8), and III (n = 7).[8] Type I AAF was characterized by the presence of single broad wavefronts propagating without significant conduction delay. Type II AAF was characterized either by single waves associated with a considerable amount of conduction block and/or conduction slowing or the presence of 2 wavelets. Type III AAF was characterized by the presence of 3 or more wavelets associated with areas of slow conduction and multiple arcs of conduction block. A more detailed description of this study population has been given previously.[8]

The remaining 23 patients (14 males, 64 ± 9 years of age) underwent cardiac surgery for valvular heart disease (mitral valve: n = 18; aortic valve: n = 2). A more detailed description of these patients has been given previously.[12,13] Coronary artery disease was present in 9 patients. Left atrial dimensions and left ventricular ejection fraction estimated by transthoracic echocardiography were 58 ± 9 mm and 50% ± 12%, respectively. The time interval between the first documentation of an AF episode and the moment of cardiac surgery was at least 1 year (long-standing persistent atrial fibrillation [LSPAF] group). The mapping protocol was approved by the Institutional Review Board of Maastricht University, and all patients provided written informed consent.

MAPPING OF AF. Epicardial recordings were acquired before patients were put on cardiopulmonary bypass. In the AAF patients, AF was induced by programmed electrical stimulation using electrodes sutured to the right atrial appendage. The right atrial free wall was mapped with a spoon shaped electrode, containing 244 unipolar electrodes (diameter 0.3 mm, interelectrode distance 2.25 mm, mapping area 36 × 36 mm). This device was held manually on the middle of the right atrial free wall. A silver plate positioned inside the thoracic cavity served as the indifferent electrode. Unipolar fibrillation electrograms and a surface electrocardiogram lead were stored on a computer disk for offline analysis (amplification: gain 1,000;

ABBREVIATIONS AND ACRONYMS

AF = atrial fibrillation

AAF = acute atrial fibrillation

AFCL = atrial fibrillation cycle length

CV = conduction velocity

LAT = local activation time

LDH = local directional heterogeneity

LSPAF = long-standing persistent atrial fibrillation

FIGURE 1 Typical Example of Acute AF Type III

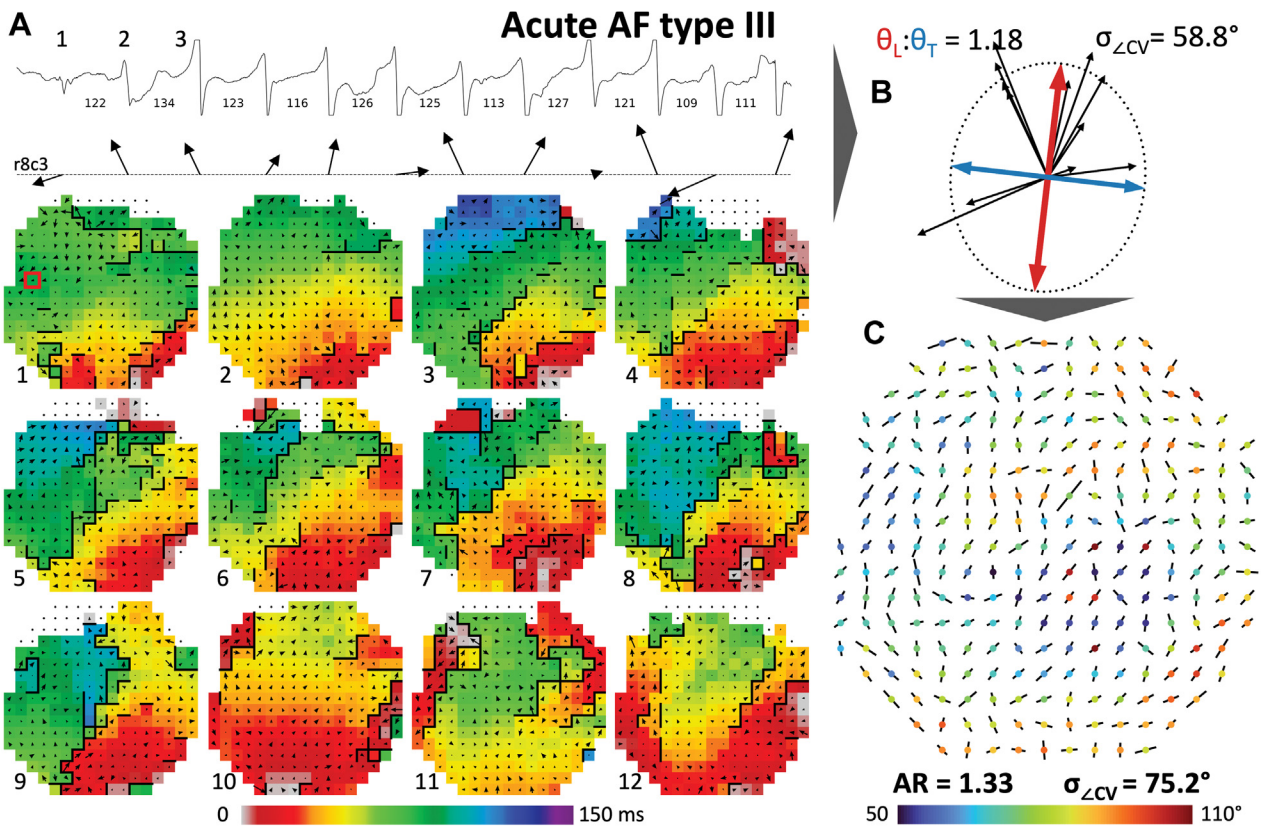

(A) A 1,442-ms-duration segment of a unipolar fibrillation electrogram (electrode r8c3) containing 12 consecutive beats of acute atrial fibrillation (AF) type III. The numbers in between the potentials indicate the beat-to-beat fibrillation intervals (in ms). Corresponding conduction velocity (CV) vectors and consecutive color-coded activation maps are shown below the electrogram. Thick black lines in the activation maps correspond with conduction block according to a time difference between adjacent electrodes of ≥12 ms. Black arrows represent the direction and magnitude of local CV. Colored squares are empty when there was no valid CV vector or when the CV was 0 cm/s. White squares with a black dot represent electrograms without a valid local activation time within the time window of the fibrillation wave. (B) An ellipse is fitted through all available local CV vectors at a specific electrode. Conduction in perpendicular directions along the major and minor axis of the fitted ellipse represent the longitudinal and transverse CV (red and blue arrows), respectively. The ratio between the 2 axes of the ellipse was used to assess the degree of local anisotropy in conduction. The variability of propagation directions is determined by the standard deviation of all local propagation angles at a specific electrode. (C) The anisotropy map shows the anisotropy ratio (AR) for every electrode. Orientation of the lines indicates the direction of the longitudinal CV and the length of the lines indicates the degree of local anisotropy. The color of the dots represent the degree of temporal variability of local propagation directions. A colorblind-friendly version of this figure can be found in Supplemental Figure 1. c = column; r = row; $\sigma_{\angle CV}$ = standard deviation of the local propagation angles; θ_L = longitudinal conduction velocity; θ_T = transverse conduction velocity.

filtering: bandwidth 1-500 Hz; sampling rate: 1 kHz; analog-to-digital conversion: 12 bits).

DATA ANALYSIS. In each patient, 4 to 20 seconds of AF were semi-automatically analyzed (9 ± 4 seconds) using specialized custom-made mapping software. Local activation times (LATs) were detected automatically and defined as the steepest negative slope of an atrial potential. All annotations were manually checked with consensus of 2 investigators. At each electrode, fibrillation intervals were assessed by measuring the time between activations by consecutive fibrillation waves (**Figures 1A and 2A**). Median atrial fibrillation cycle length (AFCL) was determined from all fibrillation intervals recorded by the 244 unipolar electrodes.

QUANTIFICATION OF CV. Based on the 244 simultaneously recorded electrograms, local CV during AF was measured by construction of CV vectors in areas of 3 × 3 electrodes (4.5 × 4.5 mm). In line with prior studies, local effective CV was then computed using discrete velocity vectors.[10] LATs of electrode pairs surrounding the center electrode

FIGURE 2 Example of Long-Standing Persistent AF

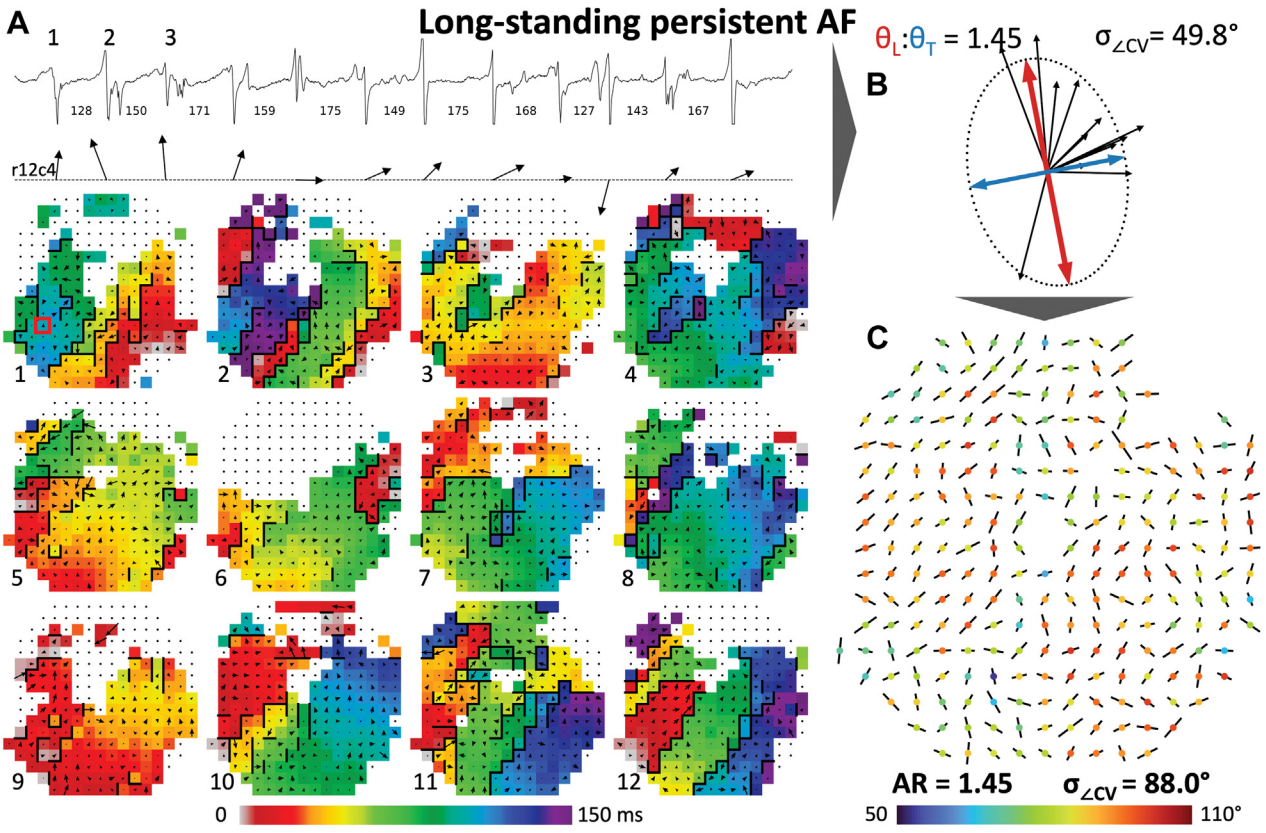

(A) A 1,972-ms-duration segment of a unipolar fibrillation electrogram (r12c4) containing 12 consecutive beats of long-standing persistent AF. The numbers in between the potentials indicate the beat-to-beat fibrillation intervals (in ms). Corresponding CV vectors and consecutive color-coded activation maps are shown below the electrogram. Twelve consecutive color-coded activation maps corresponding to the recording shown in the upper left panel. Thick black lines in the activation maps correspond with conduction block according to a time difference between adjacent electrodes of ≥12 ms. Black arrows represent the direction and magnitude of local CV. Colored squares are empty when there was no valid CV vector or when the CV was 0 cm/s. White squares with a black dot represent electrograms without a valid LAT within the time window of the fibrillation wave. (B) An ellipse is fitted through all available local CV vectors at a specific electrode. Conduction in perpendicular directions along the major and minor axis of the fitted ellipse represent the longitudinal and transverse CV (red and blue arrows), respectively. The ratio between the 2 axes of the ellipse was used to assess the degree of local anisotropy in conduction. The variability of propagation directions is determined by the standard deviation of all local propagation angles at a specific electrode. (C) The anisotropy map shows the AR for every electrode. Orientation of the lines indicates the direction of the longitudinal CV and the length of the lines indicates the degree of local anisotropy. The color of the dots represent the degree of temporal variability of local propagation directions. A colorblind-friendly version of this figure can be found in Supplemental Figure 2. Abbreviations as in **Figure 1**.

(longitudinal, transverse, and diagonal) were used to calculate the mean velocity in horizontal (x) and vertical (y) directions. Only valid LATs within a time window of $\Delta t_{max} = 12$ ms were used, corresponding to the conduction block threshold as described by Allessie et al.[12] In order to increase the reliability of the CV estimate, only CVs with at least 3 estimates in both the horizontal and vertical direction were included. The magnitude of each vector was calculated to represent the CV independently of the propagation direction angle. To avoid inclusion of far-field potentials, areas corresponding to a mean CV of 0 cm/s were excluded.

In order to quantify the local spatial irregularity in CV vectors, the amount of LDH in CV vectors was determined as previously described.[11] A local CV vector was indicated as directional heterogeneous when the local propagation angle differed more than 50% from the mean of all surrounding local propagation angles and/or the local speed was at least 50% slower than the geometric mean of all surrounding velocities. The amount of LDH was then calculated as the proportion of all CV vectors.

JACC: CLINICAL ELECTROPHYSIOLOGY VOL. 10, NO. 7, 2024
JULY 2024:1592-1604

Spatial dispersion of the parameters was calculated for each individual patient using the 5th, 50th, and 95th percentiles as: $(P_{95} - P_5)/P_{50}$. The temporal variability of local CV was measured by the standard deviation of all CV vectors per electrode. The variability of local propagation angles was computed for every electrode by using the Yamartino method.[14] For each electrode, the most frequently encountered local propagation direction was calculated by using the circular mean of all local propagation angles.

CONSTRUCTION OF ANISOTROPY MAPS. Local anisotropy in conduction was measured by fitting an ellipse through all local CV vectors obtained during the recording, as previously described by Fitzgibbon et al[15] and Halíř and Flusser, and illustrated in the **Central Illustration**.[16] The major (longest diameter) and minor axes of the fitted ellipse were assigned as longitudinal and transverse CVs, respectively, which corresponds to the directions of the fastest and slowest conduction. The ratio between the 2 axes was used to assess the degree of local anisotropy in conduction at each electrode (**Figures 1B and 2B**). An anisotropy map was then constructed by plotting the anisotropy ratio at every electrode (**Figures 1C and 2C**). The orientation of the lines indicates the direction of the fastest local CV and the length indicates the local anisotropy ratio. This method has previously been validated by pacing from 4 different directions and comparing the rotation angle of the fitted ellipse with the direction of the major pectinate muscles obtained by macrophotography.[17]

STATISTICAL ANALYSIS. Normally distributed data are expressed as mean ± SD and analyzed with a Student's *t* test. Non-normally distributed data are expressed as median (Q1-Q3) and analyzed with a Mann-Whitney *U* test. Categorical data are expressed as numbers (percentages), and analyzed with a chi-square or Fisher exact test when appropriate. Linear regression models were used to calculate correlation between the parameters. Also, linear regression models were used to assess the correlation between each of the parameters and AF severity. A P value of <0.05 was considered statistically significant.

RESULTS

MAPPING DATA CHARACTERISTICS. A total database of 2,798 fibrillation maps and 478,674 unipolar fibrillation potentials (9,972 ± 4,027 per patient) were analyzed. From these potentials, 449,307 (93.9%) CV vectors were estimated (92.5% ± 6.5% per patient), resulting in 10,567 fitted ellipses (AAF: 226 ± 27 per patient vs LSPAF: 213 ± 35 per patient; $P = 0.158$). The percentage of estimated CV vectors was higher in the AAF group (AAF: 96.3% ± 3.2% vs LSPAF: 88.4% ± 6.7%; $P < 0.001$), while more CV estimates were excluded in the LSPAF due to a CV of 0 cm/s (AAF: 0.14% [Q1-Q3: 0.09%-0.30%] vs LSPAF: 0.28% [Q1-Q3: 0.21%-0.83%]; $P = 0.041$). The average AFCL in all patients was 170 ± 35 ms and was longer in LSPAF patients (AAF: 158 ± 24 ms [range 119-215 ms] vs LSPAF: 182 ± 40 ms [range 122-308 ms]; $P = 0.014$).

EXAMPLE OF AAF AND LSPAF. Twelve consecutive fibrillation maps from 2 different patients from the AAF (type III) and LSPAF groups are shown in **Figures 1A and 2A**, respectively. As described by Konings et al,[8] type III AAF is most complex and characterized by multiple wavelets associated with areas of slow conduction (<10 cm/s) and multiple arcs of conduction block. Although in both patients almost all maps showed multiple wavelets separated by lines of functional conduction block, the LSPAF patient was characterized by a higher number of small wavelets propagating in different directions (52.9 vs 36.0 wavelets/s).

In both patients, a CV vector is visualized for each activated electrode in each of the activation maps. Despite the high complexity of the fibrillatory process in both patients, still a high amount of local effective CVs could be estimated by the algorithm (AAF patient: 97.8%; LSPAF patient: 92.6% of potentials). Both patients were characterized by a range of local CV estimates, including local areas with high velocities >100 cm/s (AAF patient: 67.3 cm/s [Q1-Q3: 26.4-135.0 cm/s] and LSPAF patient: 66.7 cm/s [Q1-Q3: 23.5-142.3 cm/s]). In the LSPAF patient, there were more prominent directional differences in CV. For instance, 2 fibrillation waves locally propagating in perpendicular directions (**Figure 2A**, vectors of beats 2 and 6) showed an effective CV of 111.6 and 72.7 cm/s, respectively. After fitting an ellipse on the 12 CV vectors, it resulted in a local anisotropy ratio of 1.45, as illustrated in **Figure 2B**. In the AAF patient, 2 fibrillation waves locally propagating in perpendicular directions (**Figure 1A**, vectors of beats 2 and 6) showed an effective CV of 72.7 and 61.4 cm/s, respectively, resulting in a local anisotropy ratio of 1.18, as illustrated in **Figure 1B**. Although a range of local conduction anisotropy was found in both patients, the LSPAF patient was characterized by a higher average anisotropy ratio (AAF patient: 1.33 [Q1-Q3: 1.01-1.97] vs LSPAF patient: 1.45 [Q1-Q3: 1.02-2.27]; $P = 0.001$). Also, there was a larger temporal

FIGURE 3 **Distribution of CV During Various Types of AF**

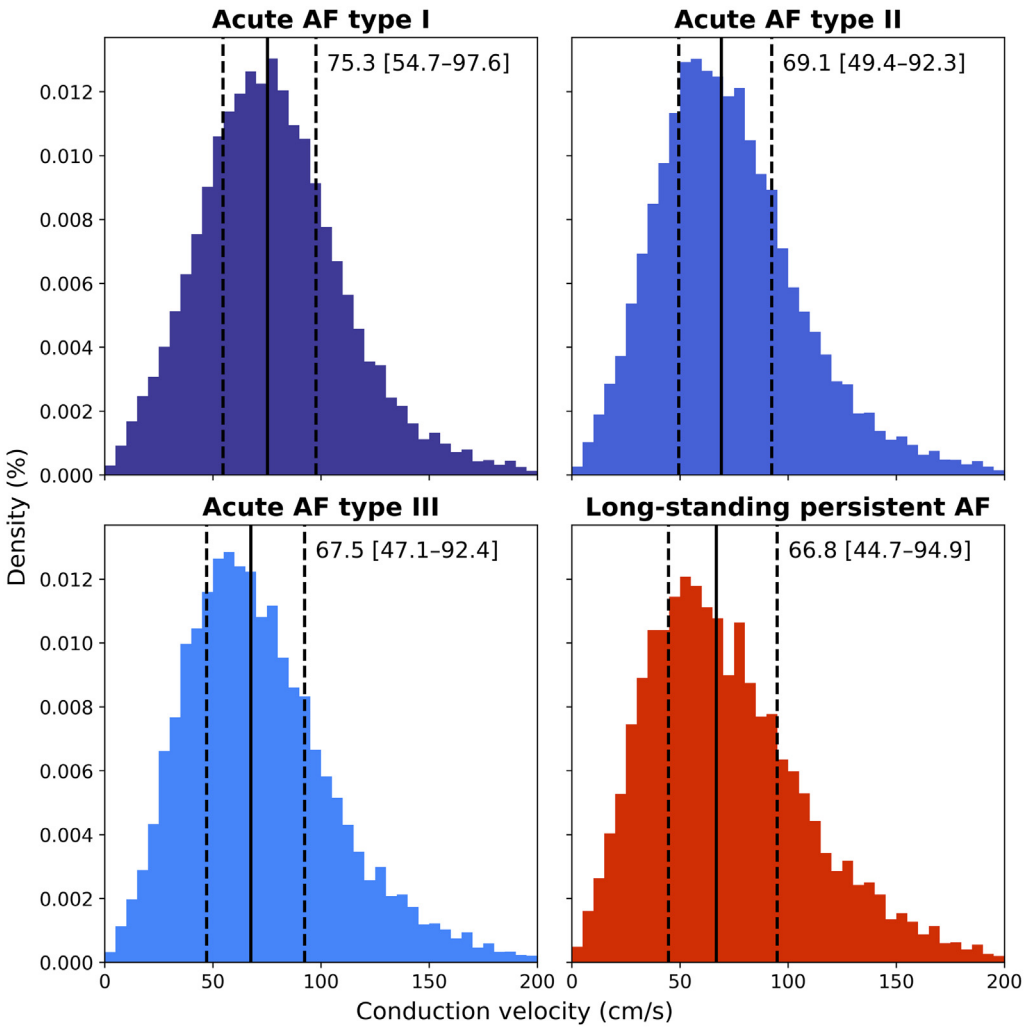

Histograms of all CV estimations per AF type ($n_{\text{acute AF type I}} = 137{,}008$; $n_{\text{acute AF type II}} = 89{,}852$; $n_{\text{acute AF type III}} = 78{,}089$; $n_{\text{long-standing persistent AF}} = 195{,}581$). Although CV gradually decreased with increasing AF severity, in all AF types, still relatively high CV estimates >100 cm/s could be found. Abbreviations as in Figure 1.

variation of local propagation directions in the LSPAF patient, as illustrated in Figures 1C and 2C. In the patient with type III AAF, the standard deviation of local propagation angles ranged between 52.7° and 94.9° (mean 75.2°), while it ranged from 69.8° to 100.0° (mean 88.0°) in the LSPAF patient ($P < 0.001$). AF was therefore more chaotic in the LSPAF patient.

SPATIOTEMPORAL DISPERSION OF LOCAL CV. Relative frequency distribution histograms of all CV estimations per AF type are visualized in Figure 3. As can be seen, CV gradually decreased with increasing AF severity. However, in all AF types, still relatively high CV estimates >100 cm/s could be found.

Comparing the averaged median CV between the AAF and LSPAF group, CV during LSPAF was lower than during AAF (AAF: 71.5 ± 6.8 cm/s vs LSPAF: 67.6 ± 5.6 cm/s; $P = 0.037$). Also, as listed in Table 1, averaged CV decreased with increasing AF complexity ($r = -0.46$, $P < 0.001$), although there was no difference between AAF type III and LSPAF ($P = 0.757$). There was no correlation between the AFCL and median CV ($r = 0.07$, $P = 0.659$).

TABLE 1 Conduction Properties During Various Types of AF

	AAF						
	Type I (n = 10)	Type II (n = 8)	Type III (n = 7)	Total (N = 25)	LSPAF (n = 23)	*P* Value	r
Number of ellipses	240 ± 8	218 ± 35	216 ± 25	226 ± 27	213 ± 35	0.158	
Median CV, cm/s	75.9 ± 6.2	70.1 ± 6.2	66.9 ± 3.7	71.5 ± 6.8	67.6 ± 5.6	0.037	−0.46[a]
CV dispersion	1.42 ± 0.17	1.63 ± 0.17	1.77 ± 0.12	1.59 ± 0.21	1.95 ± 0.17	<0.001	0.78[a]
Temporal variability CV, cm/s	30.0 ± 5.0	32.2 ± 4.2	34.7 ± 2.8	32.0 ± 4.7	38.5 ± 3.3	<0.001	0.67[a]
Temporal variability propagation angle, °	58.7 ± 13.4	73.1 ± 12.9	86.8 ± 6.0	71.2 ± 16.3	83.7 ± 8.6	0.002	0.65[a]
LDH, %	16.5 ± 3.8	20.4 ± 3.6	23.2 ± 2.3	19.6 ± 4.4	26.0 ± 3.4	<0.001	0.74[a]
Longitudinal CV, cm/s	95.7 ± 7.8	92.4 ± 7.6	94.1 ± 5.2	94.2 ± 7.2	100.8 ± 8.5	0.006	0.31
Transverse CV, cm/s	69.8 ± 5.7	67.8 ± 5.0	66.0 ± 4.1	68.1 ± 5.3	66.8 ± 4.3	0.355	−0.23
Anisotropy ratio	1.37 ± 0.08	1.36 ± 0.04	1.43 ± 0.05	1.38 ± 0.07	1.51 ± 0.14	<0.001	0.51[a]
Anisotropy ratio dispersion	0.61 ± 0.13	0.68 ± 0.08	0.79 ± 0.18	0.68 ± 0.15	0.86 ± 0.18	<0.001	0.55[a]

Values are n or mean ± SD. The *P* values indicate significance between the total of the AAF group and the LSPAF group. The correlation coefficients represent the relation between AF severity and the parameters. [a]Statistical significance of the correlation <0.001.

AAF = acute atrial fibrillation; AF = atrial fibrillation; CV = conduction velocity; LDH = local directional heterogeneity; LSPAF = long-standing persistent atrial fibrillation.

There was a larger dispersion (AAF: 1.59 ± 0.21 vs LSPAF: 1.95 ± 0.17; $P < 0.001$) and temporal variability of CV (AAF: 32.0 ± 4.7 cm/s vs LSPAF: 38.5 ± 3.3 cm/s; $P < 0.001$) during LSPAF. Dispersion in CV significantly increased with increasing AF complexity (r = 0.78, $P < 0.001$), with LSPAF having the largest dispersion even compared with AAF type III (1.95 ± 0.17 vs 1.77 ± 0.12; $P = 0.007$). There was also an increasing trend in temporal variability of CV with increasing AF complexity in the AAF group (r = 0.67, $P < 0.001$). Still, the temporal variability of CV was largest during LSPAF compared with all types of AAF ($P < 0.007$) (Table 1).

TEMPORAL VARIABILITY OF LOCAL PROPAGATION DIRECTIONS. The average standard deviation of the local propagation angles is visualized for every AAF and LSPAF patient in Figure 4. LSPAF patients were characterized by less stable vector fields in the fibrillation maps, as the average standard deviation of the local propagation angles at each electrode in these patients was larger than during AAF (AAF: 71.2° ± 16.3° vs LSPAF: 83.7° ± 8.6°; $P = 0.002$).

The smallest average standard deviations of local propagation angles were found during AAF type I (58.7° ± 13.4°; $P < 0.022$), followed by AAF type II (73.1° ± 12.9°; $P < 0.016$). The average standard deviation of the local propagation angles was comparable between AAF type III and LSPAF ($P = 0.392$). AAF type III and LSPAF were therefore most disorganized.

LOCAL DIRECTIONAL HETEROGENEITIES. In both the AAF and LSPAF groups, a considerable amount of LDH was found, as illustrated in Figure 5. In AAF patients, the amount of LDH ranged from 10.7% to 26.8% (19.6% ± 4.4%) and in the LSPAF patients from 19.4% to 33.3% (26.0% ± 3.4%). The amount of LDH was considerably higher during LSPAF ($P < 0.001$). There was no correlation between the AFCL and the amount of LDH (r = 0.05, $P = 0.749$). However, patients with slower median CV were characterized by a higher amount of LDH (r = −0.56, $P < 0.001$).

The amount of LDH increased with AF severity (r = 0.74, $P < 0.001$); it was largest during LSPAF (26.0% ± 3.4%; $P < 0.028$) and smallest during AAF type I (16.5% ± 3.8%; $P < 0.027$).

DIRECTIONAL DIFFERENCES IN CV. The longitudinal and transversal CV for every AAF and LSPAF patient is demonstrated in Figure 6. Within the AAF and LSPAF groups, there was considerable interindividual variation in both longitudinal and transverse CV. Longitudinal CV during LSPAF was higher than during AAF (AAF: 94.2 ± 7.2 cm/s vs LSPAF: 100.8 ± 8.5 cm/s; $P = 0.006$), while transverse CV was comparable between both groups (AAF: 68.1 ± 5.3 cm/s vs LSPAF: 66.8 ± 4.3 cm/s; $P = 0.355$).

There were no clear differences in longitudinal and transverse CV between the different types of AAF and LSPAF, while there was a trend to a decrease of transverse CV with increasing AF complexity.

The direction of the longitudinal axis did frequently not correspond to the mostly encountered local propagation direction. In all patients, the average absolute difference between both angles was 44.0° ± 4.2° and did not differ between the AAF and LSPAF groups (AAF: 44.3° ± 5.3° vs LSPAF: 43.7° ± 2.4°; $P = 0.591$).

FIGURE 4 Temporal Variability of Local Propagation Directions

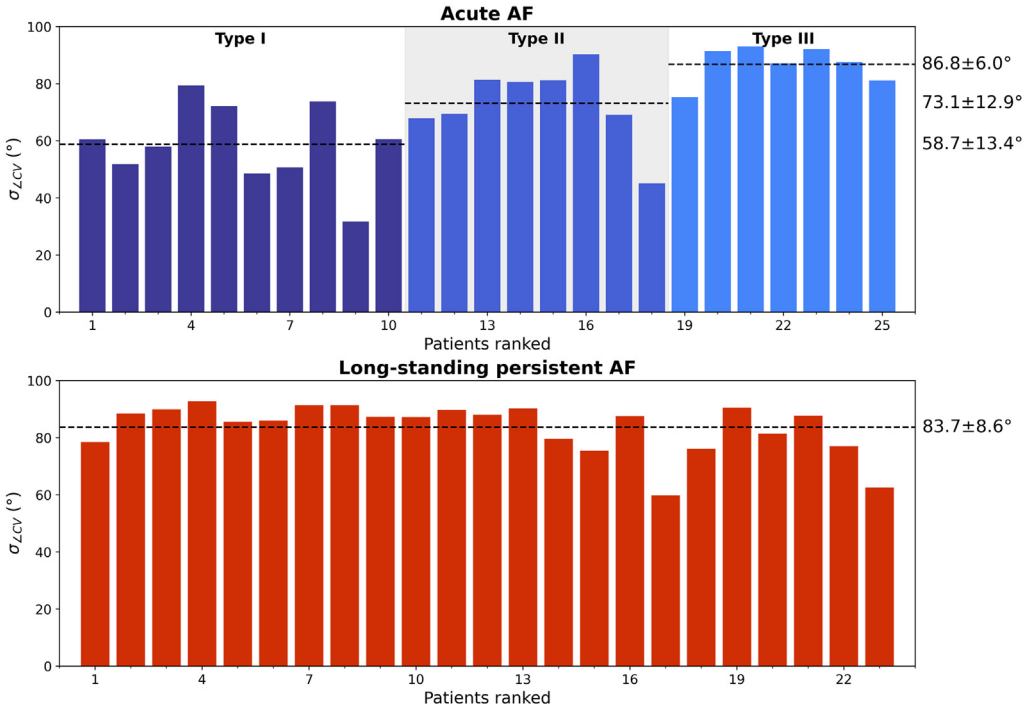

Average standard deviation of the local propagation angles is shown for every acute atrial fibrillation (AAF) (top) and long-standing persistent AF (bottom) patient separately, ranked according to the average AF cycle length. The AAF patients were subdivided according to the AF complexity (type I, II, or III). During long-standing persistent AF, the average standard deviation of the local propagation angles was higher than AAF types I and II but similar to AAF type III. Abbreviations as in Figure 1.

ANISOTROPY RATIO. The anisotropy ratio in the AAF patients ranged from 1.27 to 1.54 (1.38 ± 0.07) and in the LSPAF patients from 1.34 to 1.93 (1.51 ± 0.14), as illustrated in Figure 6. Although there was overlap in the degree of anisotropy between the AAF and LSPAF group, the anisotropy ratio was higher during LSPAF ($P < 0.001$). The dispersion of anisotropy ratios was also larger in LSPAF patients (AAF: 0.68 ± 0.15 vs LSPAF: 0.86 ± 0.18; $P < 0.001$). There was a moderate correlation between the anisotropy ratio and AFCL (r = 0.39, $P = 0.006$) and the amount of LDH (r = 0.35, $P = 0.014$).

The anisotropy ratio in LSPAF patients was comparable with AAF type III ($P = 0.120$), and larger than AAF types I and II ($P = 0.005$ and $P = 0.006$, respectively). There was also no difference in anisotropy ratio between AAF type I and II ($P = 0.774$).

DISCUSSION

In this study, we demonstrated for the first time that increasing complexity of AF was associated with increased spatiotemporal variability of local CV vectors, local conduction heterogeneity, and anisotropy ratio. By using these novel mapping parameters, we demonstrated that LSPAF could potentially be discriminated from the most complex type of AAF (type III) by a larger CV dispersion, higher temporal variability of CV, and larger amount of LDH.

EFFECTIVE CV ESTIMATION DURING AF. Data on CV during AF is scarce as estimation of CV is very difficult during nonstable patterns of activation. This is mainly due to the fact that the number of recording electrodes is often limited and sequential mapping is impossible during AF. Therefore, a high-density (grid) multielectrode array is required to accurately acquire local electrograms for CV estimation. Also, challenges in LAT assignment due to fractionation, low voltage, multiple wavefronts, wavefront collision, or wavefronts taking complicated small paths hamper global CV estimation.[18] Hence, only local methods for CV can be applied in these complex cases. As during AF

FIGURE 5 LDH in CV Vectors

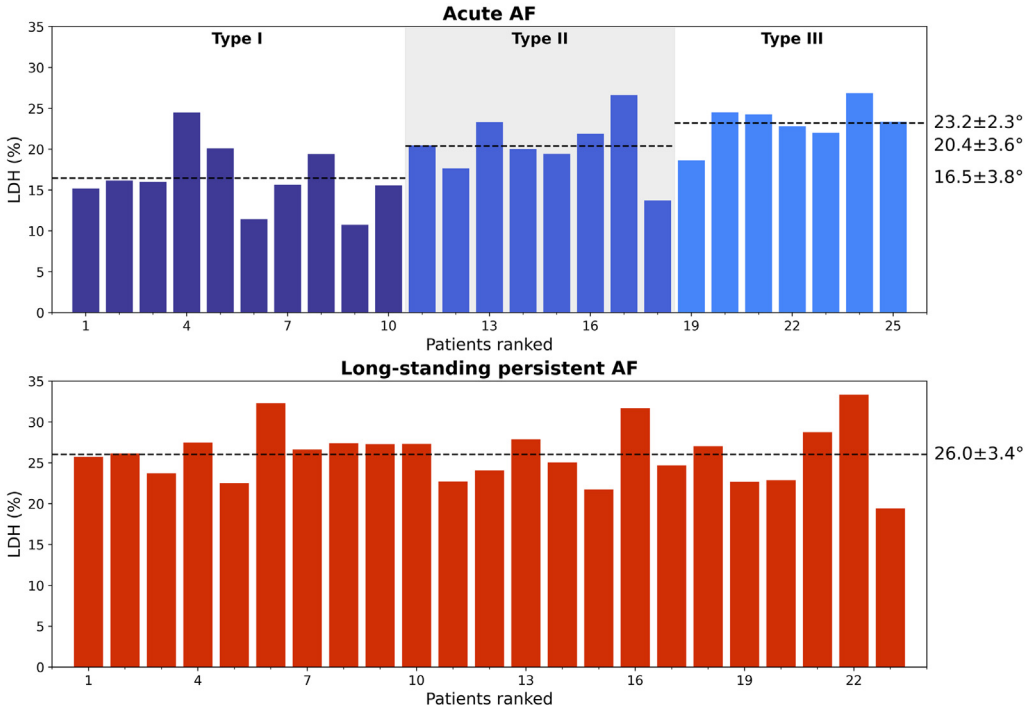

The amount of local directional heterogeneity (LDH) is shown for every AAF (top) and long-standing persistent AF (bottom) patient separately, ranked according to the average AF cycle length. The AAF patients were subdivided according to the AF complexity (type I, II, or III). During long-standing persistent AF, the amount of LDH was higher than AAF types I, II, and III. Abbreviations as in Figures 1 and 4.

there may be multiple wavefronts with short wavelengths, the spatial resolution of the electrodes should also be sufficient.[19] This is the reason why data on CV during AF are often limited to experimental studies using animal models. However, with the increasing usage of multielectrode grid catheters during endocardial electroanatomical mapping procedures, it is expected that our approach can be used during standard electrophysiologic procedures in the near future. This study provides the first insights into high-resolution CV estimation during AAF and LSPAF in humans.

INHOMOGENEITY IN CONDUCTION. Propagation of an electrical impulse is altered when active or passive cell membrane properties are affected. CV of fibrillation waves in the LSPAF patients was significantly lower with increased spatiotemporal variability compared with the AAF patients. Although a decrease in CV is known to be rate dependent, we did not find a correlation between CV and AFCL. CV during LSPAF was reduced compared with the AAF patients despite the higher longitudinal CV. This was caused by a large number of local CV vectors in other directions than the fastest direction, which resulted in a lower average CV. Therefore, it is likely that propagation of wavefronts depends more on the macroscopic atrial anatomy, whereas local CVs are more determined by the local fiber orientation.[20] Strands of viable myocardial tissue are still present in LSPAF patients, resulting in areas with fast local conduction. Due to an increased number of functional and structural barriers separating these strands, LSPAF will be more complex with more heterogeneous conduction. In the goat model of AF, Maesen et al[20] demonstrated that left atrial CV was lower in goats with persistent AF compared with those with AAF. They also found similar results on the discrepancy between the fastest and most occurring conduction direction. Local CV during AAF in human has only previously been described by Houben et al.[21] Although the average CV was comparable with our current study, they found a limited number of high velocities (>100 cm/s). This can be easily explained by the different CV estimation method that was used; as we previously

FIGURE 6 Directional Differences in CV

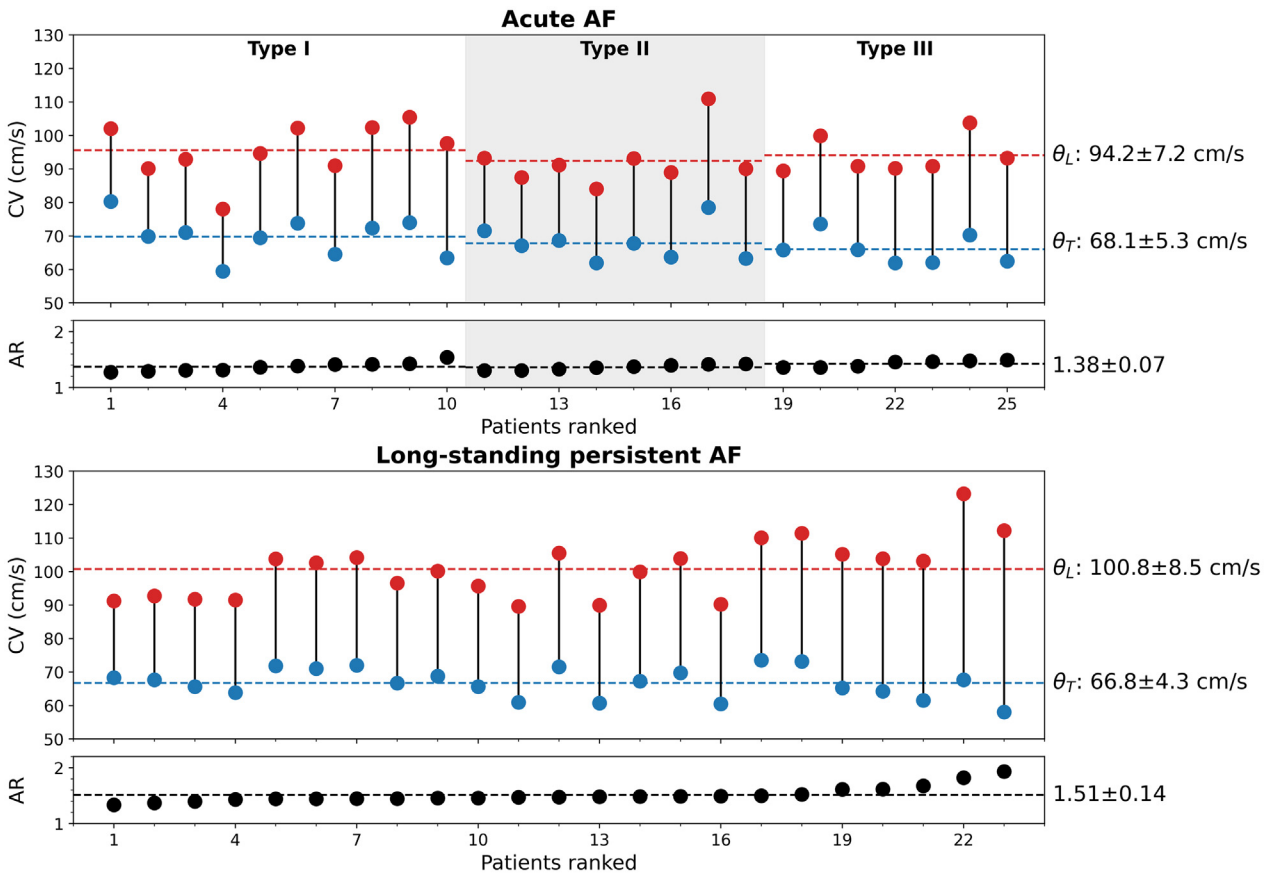

Longitudinal and transverse CV and conduction anisotropy ratio for every AAF (top) and long-standing persistent AF (bottom) patient separately, ranked according to the individual average AR. The AAF patients were subdivided according to the AAF complexity (type I, II, or III). During long-standing persistent AF, average longitudinal CV and the degree of conduction anisotropy was higher. Abbreviations as in Figures 1 and 4.

demonstrated, it was less efficient in estimating CVs, particularly in case of small wavefronts.[10]

Impairment of wavefront propagation can be the result of: 1) remodeling of cellular connections; 2) reduced membrane excitability caused by a decrease in the inward sodium current; 3) source-to-sink mismatches caused by inhomogeneous tissue volumes or wavefront curvature; and 4) tissue damage resulting in fibrosis.[22,23] Regional differences in membrane excitability can also be caused by a spatial dispersion in refractoriness and action potential duration, which are particularly present in patients with AF.[24-26] Wavefronts conducting across this heterogeneous atrial myocardium can therefore be locally distorted, which can be measured as local irregularities in CV vector maps (LDH).[11] Recently, we demonstrated in patients with structural heart disease undergoing epicardial mapping that the degree of LDH during sinus rhythm was smallest in the right atrium.[11] In the present study, we demonstrated that a higher degree of LDH is present during AF at the right atrium, even in AAF patients with normal-sized atria. Furthermore, the degree of LDH increased with AF complexity, and most LDH was therefore found in patients with LSPAF. With AF-related structural and electrical remodeling, local conduction becomes more and more impaired, leading to an increasing complexity in the fibrillatory process (Figure 2).[12,13,20,27,28]

CARDIAC ANISOTROPY. Another major determinant of myocardial conduction is cardiac anisotropy, which is considered to be arrhythmogenic, as it contributes to both initiation and perpetuation of AF.[3,9,29] Anisotropy is the property of directional dependence, meaning that electrical conduction is much faster along the longitudinal direction of myocardial

CENTRAL ILLUSTRATION **Epicardial CV and Anisotropic Properties of Fibrillation Waves in Patients With AAF and LSPAF**

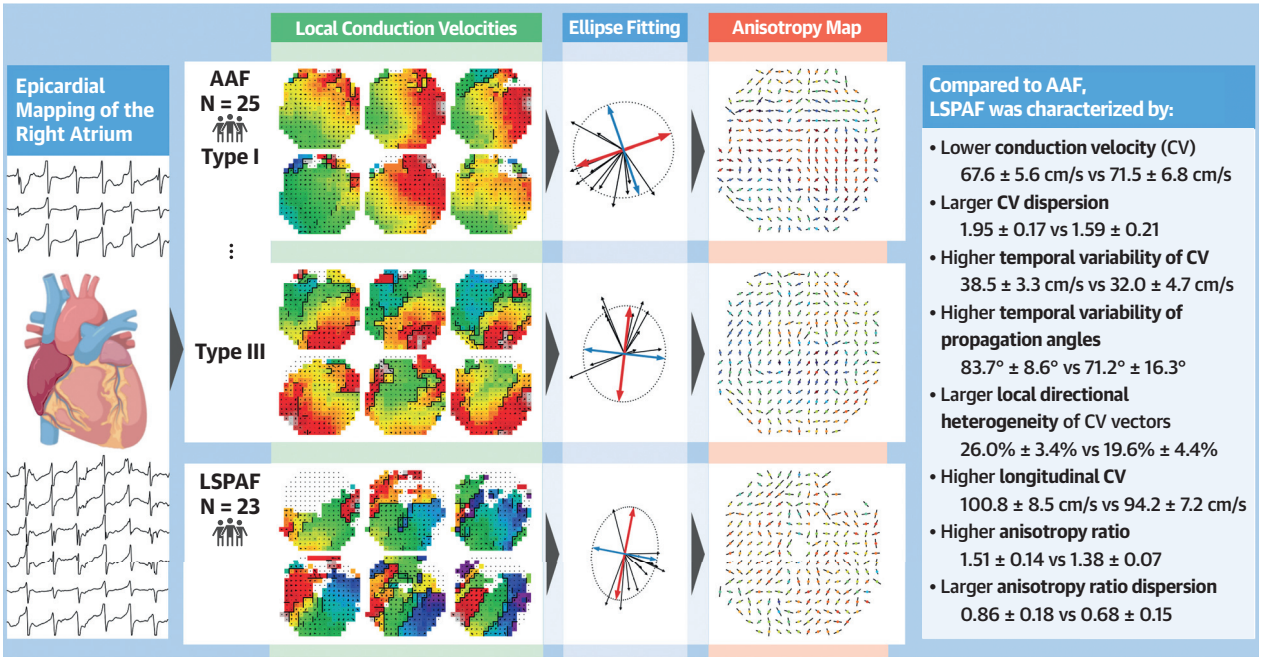

van Schie MS, et al. JACC Clin Electrophysiol. 2024;10(7):1592-1604.

Epicardial mapping of the right atrium is performed in patients with acute atrial fibrillation (AAF) or long-standing persistent atrial fibrillation (LSPAF). Conduction velocity (CV) maps of the fibrillation waves are constructed. For each electrode, an ellipse is fitted from which anisotropy maps are created. CV and anisotropy characteristics of the fibrillation waves are compared between the groups.

fibers than in transverse direction.[1] Anisotropic conduction is the result of the shape and size of the cardiomyocyte, connectivity, arrangement, and density of intercellular connections.[30] Altered cell-to-cell communication and tissue damage can result in a discontinuous distribution of conduction properties (nonuniform anisotropy), leading to unidirectional block and re-entry. Although high anisotropy ratios (ranging up to 9.8)[3] have been measured in isolated human atrial tissue, in contrast, we demonstrated relatively low anisotropy ratios in the RA during both AAF and LSPAF. These relatively low anisotropy ratios during AF were also found by Maesen et al[20] in the left atrial free wall of goats. However, they did not find a difference in anisotropy ratio between AAF and persistent AF. In contrast, we demonstrated that the anisotropy ratio at the right atrium was higher in LSPAF patients compared with AAF patients. Other studies also demonstrated enhanced anisotropic conduction in the right atrium in patients with chronically stretched atria secondary to mitral valve stenosis and in patients undergoing surgical AF ablation.[31,32] In addition, we also demonstrated a larger spatial variety of anisotropic properties in LSPAF patients. Therefore, the heterogeneously increased anisotropic properties of atrial tissue seen during LSPAF contribute to AF persistence.

Cardiac anisotropy is also influenced by ageing and structural heart diseases. Patients in the LSPAF group were significantly older than patients in the AAF group. Spach and Dolber[3] demonstrated that aging is associated with an increase in interstitial fibrosis resulting in a decrease in side-to-side electrical coupling thereby giving rise to nonuniform anisotropy. Also, all LSPAF patients had valvular heart disease. Augmentation of atrial fibrosis, due to chronic stretch caused by valvular heat disease or alterations of atrial structure by AF itself could account for a higher incidence of conduction abnormalities during LSPAF.[33,34]

STUDY LIMITATIONS. As a historical dataset of AF patients was used for this study, no histological examination could be performed. Therefore, it remains

unknown whether the longitudinal CV truly represents the myocardial fiber direction in this population. However, previous other studies validated the proposed method to determine the anisotropy ratio and its relation to myocardial fiber direction.[9,17,21] Besides, as the same method was applied on both groups, they act as a control for one other.

CONCLUSIONS

Increasing complexity of AF was associated with increased spatiotemporal variability of local CV vectors, local conduction heterogeneity, and anisotropy ratio. By using these novel mapping parameters, we demonstrated that LSPAF could potentially be discriminated from the most complex type of AAF (type III) by a larger CV dispersion, higher temporal variability of CV, and larger amount of LDH. These observations may indicate pathological alterations of myocardial tissue underlying progression of AF.

ACKNOWLEDGMENTS The authors kindly thank their colleagues at Maastricht University for their help in collecting the historical dataset of AF electrograms at the time.

FUNDING SUPPORT AND AUTHOR DISCLOSURES

The authors have reported that they have no relationships relevant to the contents of this paper to disclose.

ADDRESS FOR CORRESPONDENCE: Dr Natasja M.S de Groot, Unit Translational Electrophysiology, Department of Cardiology, Erasmus Medical Center, Dr. Molewaterplein 40, 3015GD Rotterdam, the Netherlands. E-mail: n.m.s.degroot@erasmusmc.nl.

PERSPECTIVES

COMPETENCY IN MEDICAL KNOWLEDGE: During AAF, the right atrial free wall of young patients without structural heart disease is mainly activated uniformly by broad wavefronts with low conduction anisotropy. It is most likely that conduction in older patients with underlying cardiac diseases and dilated atria is additionally affected by alterations of the atrial structure, thereby inducing nonuniform anisotropic features. This study demonstrated for the first time that LSPAF could potentially be discriminated from the most complex type of AAF (type III) by a larger dispersion of CV, higher temporal variability of CV, and a larger amount of local heterogeneity in CV vectors. Increasing complexity of AF was associated with increased spatiotemporal variability of local CV vectors, local conduction heterogeneity, and conduction anisotropy.

TRANSLATIONAL OUTLOOK: Quantified features of local conduction heterogeneity due to pathological alterations of myocardial tissue could serve as an electrical biomarker of the degree of electrical remodeling and hence to determine the stage of AF. In our study population, patients with LSPAF were characterized by a larger dispersion of CV, higher temporal variability of CV, and a larger amount of local heterogeneity in CV vectors compared with patients with AAF without prior AF episodes. Additional studies will be required to confirm whether these observations indeed indicate pathological alterations of myocardial tissue underlying progression of AF. As high-resolution grid electrodes are more commonly used in clinical practice, the proposed parameters might also be applied during electroanatomical mapping procedures. However, application of our technique might be less suitable for noninvasive technologies such as body surface mapping.

REFERENCES

1. Kleber AG, Rudy Y. Basic mechanisms of cardiac impulse propagation and associated arrhythmias. *Physiol Rev*. 2004;84:431–488.

2. Spach MS, Dolber PC, Heidlage JF. Influence of the passive anisotropic properties on directional differences in propagation following modification of the sodium conductance in human atrial muscle. A model of reentry based on anisotropic discontinuous propagation. *Circ Res*. 1988;62:811–832.

3. Spach MS, Dolber PC. Relating extracellular potentials and their derivatives to anisotropic propagation at a microscopic level in human cardiac muscle. Evidence for electrical uncoupling of side-to-side fiber connections with increasing age. *Circ Res*. 1986;58:356–371.

4. Feng J, Yue L, Wang Z, Nattel S. Ionic mechanisms of regional action potential heterogeneity in the canine right atrium. *Circ Res*. 1998;83:541–551.

5. Simpson RJ Jr, Foster JR, Gettes LS. Atrial excitability and conduction in patients with interatrial conduction defects. *Am J Cardiol*. 1982;50:1331–1337.

6. van Schie MS, de Groot NM. Clinical relevance of sinus rhythm mapping to quantify electropathology related to atrial fibrillation. *Arrhythm Electrophysiol Rev*. 2022;11:e11.

7. Hansson A, Holm M, Blomstrom P, et al. Right atrial free wall conduction velocity and degree of anisotropy in patients with stable sinus rhythm studied during open heart surgery. *Eur Heart J*. 1998;19:293–300.

8. Konings KT, Kirchhof CJ, Smeets JR, Wellens HJ, Penn OC, Allessie MA. High-density mapping of electrically induced atrial fibrillation in humans. *Circulation*. 1994;89:1665–1680.

9. Houben RP, de Groot NM, Smeets JL, Becker AE, Lindemans FW, Allessie MA. S-wave predominance of epicardial electrograms during atrial fibrillation in humans: indirect evidence for a role of the thin subepicardial layer. *Heart Rhythm*. 2004;1:639–647.

10. van Schie MS, Heida A, Taverne Y, Bogers A, de Groot NMS. Identification of local atrial conduction heterogeneities using high-density conduction velocity estimation. *Europace*. 2021;23:1815–1825.

11. van Schie MS, Misier NLR, Razavi Ebrahimi P, et al. Premature atrial contractions promote local directional heterogeneities in conduction velocity vectors. *Europace*. 2023;25:1162–1171.

12. Allessie MA, de Groot NM, Houben RP, et al. Electropathological substrate of long-standing persistent atrial fibrillation in patients with structural heart disease: longitudinal dissociation. *Circ Arrhythm Electrophysiol*. 2010;3:606–615.

13. de Groot NM, Houben RP, Smeets JL, et al. Electropathological substrate of longstanding

persistent atrial fibrillation in patients with structural heart disease: epicardial breakthrough. *Circulation*. 2010;122:1674–1682.

14. Yamartino RJ. A Comparison of several single-pass estimators of the standard-deviation of wind direction. *J Clim Appl Meteorol*. 1984;23:1362–1366.

15. Fitzgibbon A, Pilu M, Fisher RB. Direct least square fitting of ellipses. *IEEE Trans Pattern Anal Mach Intell*. 1999;21:476–480.

16. Halíř R, Flusser J. Numerically stable direct least squares fitting of ellipses. *J WSCG*. 1998;6:125–132.

17. Eijsbouts SC, Houben RP, Blaauw Y, Schotten U, Allessie MA. Synergistic action of atrial dilation and sodium channel blockade on conduction in rabbit atria. *J Cardiovasc Electrophysiol*. 2004;15:1453–1461.

18. de Groot NMS, Shah D, Boyle PM, et al. Critical appraisal of technologies to assess electrical activity during atrial fibrillation: a position paper from the European Heart Rhythm Association and European Society of Cardiology Working Group on eCardiology in collaboration with the Heart Rhythm Society, Asia Pacific Heart Rhythm Society, Latin American Heart Rhythm Society and Computing in Cardiology. *Europace*. 2022;24:313–330.

19. Roney CH, Cantwell CD, Bayer JD, et al. Spatial resolution requirements for accurate identification of drivers of atrial fibrillation. *Circ Arrhythm Electrophysiol*. 2017;10:e004899.

20. Maesen B, Zeemering S, Afonso C, et al. Rearrangement of atrial bundle architecture and consequent changes in anisotropy of conduction constitute the 3-dimensional substrate for atrial fibrillation. *Circ Arrhythm Electrophysiol*. 2013;6:967–975.

21. Houben RP, Allessie MA. Processing of intracardiac electrograms in atrial fibrillation. Diagnosis of electropathological substrate of AF. *IEEE Eng Med Biol Mag*. 2006;25:40–51.

22. Spach MS, Miller WT 3rd, Dolber PC, Kootsey JM, Sommer JR, Mosher CE Jr. The functional role of structural complexities in the propagation of depolarization in the atrium of the dog. Cardiac conduction disturbances due to discontinuities of effective axial resistivity. *Circ Res*. 1982;50:175–191.

23. Spach MS, Boineau JP. Microfibrosis produces electrical load variations due to loss of side-to-side cell connections: a major mechanism of structural heart disease arrhythmias. *Pacing Clin Electrophysiol*. 1997;20:397–413.

24. Gaspo R, Bosch RF, Bou-Abboud E, Nattel S. Tachycardia-induced changes in Na+ current in a chronic dog model of atrial fibrillation. *Circ Res*. 1997;81:1045–1052.

25. Gaspo R, Bosch RF, Talajic M, Nattel S. Functional mechanisms underlying tachycardia-induced sustained atrial fibrillation in a chronic dog model. *Circulation*. 1997;96:4027–4035.

26. Fareh S, Villemaire C, Nattel S. Importance of refractoriness heterogeneity in the enhanced vulnerability to atrial fibrillation induction caused by tachycardia-induced atrial electrical remodeling. *Circulation*. 1998;98:2202–2209.

27. Eckstein J, Zeemering S, Linz D, et al. Transmural conduction is the predominant mechanism of breakthrough during atrial fibrillation: evidence from simultaneous endo-epicardial high-density activation mapping. *Circ Arrhythm Electrophysiol*. 2013;6:334–341.

28. Verheule S, Tuyls E, van Hunnik A, Kuiper M, Schotten U, Allessie M. Fibrillatory conduction in the atrial free walls of goats in persistent and permanent atrial fibrillation. *Circ Arrhythm Electrophysiol*. 2010;3:590–599.

29. Spach MS. Anisotropy of cardiac tissue: a major determinant of conduction? *J Cardiovasc Electrophysiol*. 1999;10:887–890.

30. Spach MS, Heidlage JF, Dolber PC, Barr RC. Changes in anisotropic conduction caused by remodeling cell size and the cellular distribution of gap junctions and Na(+) channels. *J Electrocardiol*. 2001;34(Suppl):69–76.

31. Wong CX, John B, Brooks AG, et al. Direction-dependent conduction abnormalities in the chronically stretched atria. *Europace*. 2012;14:954–961.

32. Krul SP, Berger WR, Smit NW, et al. Atrial fibrosis and conduction slowing in the left atrial appendage of patients undergoing thoracoscopic surgical pulmonary vein isolation for atrial fibrillation. *Circ Arrhythm Electrophysiol*. 2015;8:288–295.

33. Allessie M, Ausma J, Schotten U. Electrical, contractile and structural remodeling during atrial fibrillation. *Cardiovasc Res*. 2002;54:230–246.

34. Ausma J, Wijffels M, Thone F, Wouters L, Allessie M, Borgers M. Structural changes of atrial myocardium due to sustained atrial fibrillation in the goat. *Circulation*. 1997;96:3157–3163.

KEY WORDS atrial fibrillation, anisotropy, electrophysiology, conduction disorders, conduction heterogeneity, high-resolution epicardial mapping, induced atrial fibrillation, long-standing persistent atrial fibrillation, remodeling

APPENDIX For supplemental figures, please see the online version of this paper.